Towards a Mechanism of Function of the Viral Ion Channel Vpu from HIV-1

http://www.jbsdonline.com

Abstract

Vpu, an integral membrane protein encoded in HIV-1, is implicated in the release of new virus particles from infected cells, presumably mediated by ion channel activity of homo-oligomeric Vpu bundles.

Reconstitution of both full length Vpu_{1-81} and a short, the transmembrane (TM) domain comprising peptide Vpu_{1-32} into bilayers under a constant electric field results in an asymmetric orientation of those channels. For both cases, channel activity with similar kinetics is observed. Channels can open and remain open within a broad series of conductance states even if a small or no electric potential is applied.

The mean open time for Vpu peptide channels is voltage-independent. The rate of channel opening shows a biphasic voltage activation, implicating that the gating is influenced by the interaction of the dipole moments of the TM helices with an electric field.

Key words: Vpu; HIV-1; Membrane proteins; Ion channels; and Gating.

T. Mehnert[1]
Y. H. Lam[1]
P. J. Judge[1,2]
A. Routh[1]
D. Fischer[1]
A. Watts[1]
W. B. Fischer[1,2,§,*]

[1]Biomembrane Structure Unit

Department of Biochemistry

Oxford University

South Parks Road

Oxford OX1 3QU, UK

[2]Bionanotechnology Interdisciplinary

Research Collaboration (IRC)

Clarendon Laboratory

Department of Physics

Oxford University, Parks Road

Oxford OX1 3PU, UK

§Current address:

Institute of Biophotonics

School of Medical Science and Engineering

National Yang Ming University

Taipei, Taiwan

Introduction

The genome of the human immunodeficiency virus type-1 encodes an 81 amino acid type I integral membrane protein called Vpu (1, 2). Vpu is a non-essential protein for viral replication in certain tissue culture, but highly important *in vivo* (3). The structure of Vpu comprises of a short transmembrane (TM) domain at the N terminus and a 54 amino acid phosphorylated cytoplasmic part at the C terminus. The overall structure has been resolved with protein fragments using NMR, FTIR, and CD spectroscopy [reviewed in (4-7)] indicating the existence of three to four helices, from which one is due to the membrane spanning part of the protein. Vpu fulfills two distinct roles during the virus life cycle: (i) its cytoplasmic C-terminal domain interacts with the CD4 receptor in the endoplasmic reticulum initiating CD4 degradation (8-10) and (ii) its TM domain is responsible for an amplification of the budding rate of new virus particles (11). In the latter case, it is suggested that Vpu oligomerizes to form ion conducting channels (12).

Recently, it has been reported that Vpu associates with the TWIK related acid sensitive leakage K^+ channel (TASK) that leads to a support of viral release (13). However, this interaction with TASK might be an additional route of Vpu action. Nevertheless, the presence of Vpu in artificial lipid membrane leads to channel formation as indicated by bilayer experiments. The cannel activity of Vpu itself may affect the conformation or activity of neighboring proteins and lipids as a consequence of enabling the change of the electrochemical gradient.

Also, genomes of other viruses encode short proteins that show membrane activity and act as ion channels. Examples include M2 from Influenza A (14-16), NB and

*Phone: +886-2-2826-7394
Fax: +886-2-2823-5460
Email: wfischer@ym.edu.tw

BM2 from Influenza B (17, 18), the Kcv protein from Chlorella virus PBCV-1 (19), p7 from Hepatitis C virus (HCV) (20), 3a from the severe acute respiratory syndrome-associated coronavirus (SARS-CoV) (21), and other proteins (22, 23).

Channel activity of Vpu and its amplification of particle release have been attributed to the TM domain (10, 12, 24). This result is also based on experiments of Vpu peptides, which correspond to the TM domain and reconstituted into artificial lipid membranes.

For the short membrane spanning Vpu peptide, several questions arise: (i) does the peptide assemble/disassemble like other short membrane active peptides [reviewed in, *e.g.*, (25, 26)] such as alamethicin (27), melittin (28), or gramicidin (29) to enable ion flux or (ii) does the peptide bundle exhibits gating characteristics like neuronal ion channels. In the latter, how is gating achieved with the proposed channel/pore architecture of Vpu consisting of a longer hydrophobic stretch towards the N terminus and a short hydrophilic stretch towards the C terminus?

In the present study, full length Vpu (Vpu_{1-81}) and a peptide corresponding to the first 32 amino acids of Vpu including the TM domain (Vpu_{1-32}) have been reconstituted separately into artificial lipid membranes (30) and the effect of an external electric field on the kinetic properties of the peptide channels has been analyzed. Effects that influence or even control the gating process are discussed. Channel activity has been also shown for the peptide when reconstituted into an immobilized membrane system (31).

Materials and Methods

Protein Expression

Vpu_{1-81} was expressed as a fusion protein with glutathione-*S*-transferase using the pGex-vpu plasmid provided by Prof. P. Gage, Australia National University, Canberra, Aus.

The pGex-vpu plasmid was inserted into competent BL21 *E. coli* cells (Invitrogen) by heat shock transformation. Cells were grown in 3000ml lysogeny broth (LB) medium containing 50µg/ml ampicillin and the turbidity of the culture was followed at 600nm. Cells were induced by adding isopropyl-β-D-thiogalactopyranoside (IPTG) to a final concentration of 0.5mM when $0.45 < A_{600} < 0.55$. After four hours cells were harvested by centrifugation at 6000g for 30min at 4 °C.

Cells were washed with phosphate buffered saline (PBS) buffer (150mM NaCl, 16mM Na_2HPO_4, 4mM NaH_2PO_4) and were resuspended in 15ml Buffer I [50mM Tris/HCl pH 7.5, 100mM NaCl, 1mM NaN_3, 1mM dithiothreitol (DTT)]. 200µl of 50mg/ml lysozyme solution and 5µl DNase I were added followed by 15ml Buffer II (50mM Tris/HCl pH 7.5, 1% v/v Na deoxycholate, 1% v/v Triton-X-100, 1mM NaN_3, 1mM DTT). The mixture was incubated at room temperature for 30 minutes, sonicated for 5× 30s duty cycle 60% (MSE Scientific Instruments) and then centrifuged at 17,000 g for 30min at 4 °C.

The supernatant was discarded and the pellet resuspended in 15ml buffer III and sonicated for 5× 30s duty cycle 60% and then centrifuged at 19,000 g for 30min at 4 °C.

The pelleted inclusion bodies were washed with guanidine hydrochloride binding (GHB) buffer (6M Guanidium chloride, 0.5mM NaCl, 20mM Tris/HCl pH 7.5) and then diluted 1 in 10 into refolding buffer (50mM Tris/HCl, 0.2M NaCl, 1mM DTT, 1M non-detergent sulfobetaines (NDSB) 256) at 4 °C and the solution was slowly agitated overnight. The solution was concentrated using a 10 kDa centrifuge concentrator (Amicron) and dialyzed into Thrombin Cleavage Buffer (TCB) (50mM Tris/HCl pH 7.5, 150mM NaCl, 2.5mM $CaCl_2$, 1mM DTT).

The protein was applied to a GSTrap column [Glutathione S-Transferase (GST), Amersham biosciences] and washed with TCB pH 7.5. The protein was eluted using trichlorobutanol (TCB) + 10mM reduced glutathione and then concentrated to 1ml and dialyzed overnight into TCB pH 6.5. Cleavage of the GST-Vpu fusion protein was carried out overnight at room temperature using two units bovine thrombin (Sigma). The purity of the protein was monitored using Western blot analysis with Vpu specific polyclonal antibodies and SDS PAGE (sodium dodecyl sulfate polyacrylamide gel electrophoresissodium dodecyl sulfate polyacrylamide gel electrophoresis).

The solution was then lyophilized and resolubilized in 500ml trifluoroethanol (TFE), and then sonicated for 10 minutes on a bath sonicator. 500ml buffer B (acetonitrile + 0.1% 2,2,2-trifluoroacetic acid) was then added. The protein was purified by HPLC using a semiprep C4 column (Hichrom) and a gradient of 80% buffer A (double distilled water + 0.1% trifluoroacetic acid) 20% buffer B to 20% buffer A and 80% buffer B over the course of one hour (flow rate 3ml/minute). The solvents were removed by evaporation and lyophilization and the purified Vpu was resolubilized in TFE to a concentration of 1mg/ml.

Peptide Synthesis

Vpu_{1-32} with the sequence

MQPIPIVAIV[10] ALVVAIIIAI[20] VVWSIVIIEY[30] RK

was synthesized on a Pioneer Synthesizer from Applied Biosystems Instruments using Fmoc chemistry.

[5-(4-Fmoc-aminomethyl-3,5-dimethoxyphenoxy)valeric acid]-polyethylene glycol-polystyrene resin (Fmoc-PAL-PEG-PS resin) was used with a deprotecting solvent of 20% piperidine in N,N-dimethylformamide (DMF) and a 4-fold excess of 9-fluorenylmethoxycarbonyl-amino acids (Fmoc) with coupling reagents diiso-

Full length Vpu$_{1-81}$ **Vpu$_{1-32}$**
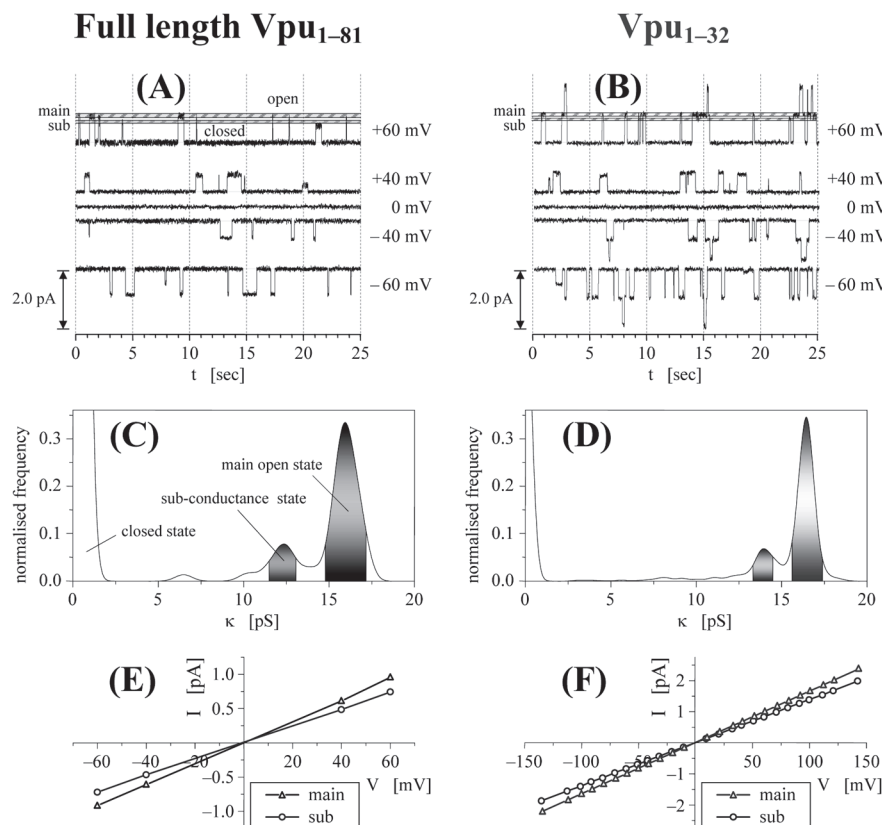
Figure 1: Examples of channel recordings from Vpu$_{1-81}$ (**A**, **C**, **E**) and Vpu$_{1-32}$ (**B**, **D**, **F**), reconstituted into bilayers (300 mM KCl, 5 mM K$^+$-HEPES, pH = 7.0). (**A**) and (**B**), representative traces at different voltages. For +60 mV the defined conductance ranges, as shown in (**C**) and (**D**), are given as shaded bars. (**C**) and (**D**), representative conductance histograms of traces comprising more than 600 events each. The variance of the Gaussian distributions is set to 0.0025 pS. (**E**) and (**F**), I/V curves of the main-conductance state and the sub-conductance state. The mean standard error for each point is smaller than the size of the symbols.

propylethylamine (DIPEA), N-hydroxybenzotriazole (HOBT), O-benzotriazole-N,N,N',N'-tetramethyl-uronium-hexafluorophosphate (HBTU), and for double coupling N-[(dimethylamino)-1H-1,2,3-trianzolo[4,5-b]pyridine-1-ylmethylene]-N-methylmethanaminium hexafluorophosphate N-oxide (HATU) or benzotriazole-1-yl-oxy-tris-pyrrolidino-phosphonium-hexafluorophosphate (PyBOP). Chemicals were obtained from Novabiochem and Applied Biosystems (Warrington, UK).

The resin was washed first with dichlormethane (DCM) and then with methanol and dried under vacuum overnight. The cleavage of the peptide from the resin was carried out using trifluoroacetic acid (TFA) in the presence of appropriate scavengers under room temperature (reaction time 5h). The combined filtrates were evaporated under N_2 gas and cold ether was added to precipitate the peptide. The precipitate was centrifuged and the solvent decanted.

The lyophilized cleavage mixture was purified by reverse-phase HPLC [high performance liquid chromatography on a C18 column (Zorbax 300SB, 4.6 × 250mm, 300 Å pore size, Hichrom)] with a gradient of a mixture of TFE in isopropanol and acetronitrile, and MilliQ water in 0.1% TFA. Elution of the peptide was followed spectroscopically at 220nm and 280nm. The exact mass of the peptide was 3544,8 Dalton on a ion MALDI spectra obtained with a Waters-Micromass TofSpec 2E time-of-flight (TOF) mass spectrometer (Waters/Micromass MS Technologies Ltd, Manchester, UK) (Figure 1B). The correct amino acid sequence of the first 8 amino acids of the peptide was analysis by automated peptide sequencing analysis on an Applied Biosystem 494A (Warrington UK) (32).

Reconstitution and Channel Recordings

A 1:4 mixture of 1-palmitoyl-2-oleoyl-_sn_-glycero-3-phosphoethanolamine (POPE) and 1,2-dioleoyl-_sn_-glycero-3-phosphocholine (DOPC) (Avanti Polar Lipids, Alabaster, US) was dissolved in chloroform, dried under N_2 gas, and resuspended in _n_-decane at 20.0mg/ml. For channel recordings, a Delrin cup chamber system was used with an aperture diameter of 150μm. After brushing lipid suspension across the aperture each chamber was filled with 1ml buffer (300mM KCl, 5mM K^+-HEPES, pH = 7.0) and the buffer level was raised and lowered until a bilayer was formed. Aliquots of 10μl of Vpu_{1-81} or Vpu_{1-32}, dissolved in TFE at 1.0mg/ml, were pipetted into the aqueous subphase in the _cis_-chamber (ground). Reconstitution was achieved by lowering and raising the buffer again in the presence of a constant negative voltage (_trans_ relative to _cis_). Experiments were performed at T = 24 ± 1 ℃. The current response was recorded using a MultiClamp 700A system from Axon Instruments (Union City, US) and data were filtered with a Bessel-8-pole low-pass-filter at 100Hz. Shut events shorter than 15ms were considered as part of a burst.

Data Analysis – Conductance Histograms

Channel data usually are significantly influenced by noise. For this reason, to obtain a more detailed distribution of the conductance states a channel can occupy, conductance histograms were created by superimposing individual, dwell-time-weighted Gaussian distribution functions, each representing one of the recorded events. For a recorded trace with N_{ev} events the conductance-histogram function $f(\kappa)$ is

$$f(\kappa) = \frac{A}{\sqrt{2\pi}\sigma} \sum_{i=1}^{N_{ev}} t_{dw,i} \exp\left[-\left(\frac{\kappa - \kappa_i}{\sigma}\right)^2\right].$$

A is a normalization constant, set so that $\int_0^\infty f(\kappa)d\kappa = 1$. In $f(\kappa)$ the _ith_ event of a recorded trace is considered by its dwell time $t_{dw,i}$ and its conductivity $\kappa_i = I_i/V$ (measured current value divided by the applied voltage). The width σ is set to a small value, uniform for all events.

Channel recording measurements with Vpu_{1-81} as well as with Vpu_{1-32} at constant voltage within a range of ±60 mV have been performed (Fig. 1A and B). Each recorded trace contains between 900 and 1600 events. The data reveal frequent channel openings to multiple conductance states between 2.4 pS and 20.2 pS (300 mM KCl, 5 mM K^+-HEPES, pH = 7.0). In both cases, channels open mostly to a main-conductance state, at 16.0 ± 1.2 pS (standard deviation) for Vpu_{1-81} and at 16.5 ± 0.9 pS for Vpu_{1-32} (Fig. 1C and D). More seldom both systems also open to a range of sub-conductance states with a second maximum at 12.3 ± 0.8 pS and at 13.9 ± 0.6 pS, respectively. These maxima will be treated in the analysis of channel kinetics as a second conductance state. As a general trend, below the main-conductance state the occurrence rate of a state decreases with lessening conductivity κ. Occasionally, conductance states with κ higher than that of the main state, up to 20 pS, are observed too. The relative rate with which the conductance states occur is independent of the applied voltage.

For both systems (Vpu_{1-81} and Vpu_{1-32}) the I/V curves of the two states show an ideal ohmic behavior regardless of the direction of the electric field (Fig. 1E and F). Based on the method chosen for reconstitution it can be presumed that Vpu_{1-81} and Vpu_{1-32} adopted a preferred orientation in the membrane during the recordings. The ohmic response, therefore, rules out any rectifying behavior or voltage gating of Vpu oligomers under physiological conditions.

Measurements on Vpu_{1-32} with continuous voltage ramps ranging between ±120 mV reveal that these channels can remain open at very small voltages and at 0 mV (Fig. 2A), and consequently that openings and closings can be caused by spontaneous conformational changes in the TM helices due to thermal motion.

Open channel events for both systems frequently show burst-like or flickering patterns (Fig. 2B) and typically last for several hundred milli-seconds. Single channel openings generally remain at a constant conductance level and direct transitions from one conductance state to another (33) (Fig. 2C) are rare and, for this reason, are not considered in the statistical analysis. For analysis, events with simultaneous openings of several channels were separated as shown in the hatched areas in Figure 2D. During events with simultaneous openings of several channels, neither a correlation between the times of opening nor between the times of closing of those channels nor between their conductance levels can be found. No repetitive sequence of states was found either, suggesting that their occurrence is random. Thus, data analysis has been performed within the Markov model.

For detailed investigations of the kinetics, the mean open time τ_O and the transition rate k_{+i} from the shut state to an open state i, channels were incorporated in a membrane with a new method: Reconstitution in the presence of a constant electric field leads to a preferred orientation of the channels as this is supported by both the greater hydrophobicity of the N-terminus of Vpu and the interaction of its TM-helix dipole moment with the external electric field.

Cumulative dwell-time histograms were derived from the recorded traces of Vpu_{1-81} and Vpu_{1-32}. As the number of channels in the membrane is indeterminate, relative open rates k_{+i} (+ stands for the open rate, - for the shut rate) from the shut state of the whole system – all channels in the bilayer – to a given conductance state were calculated, normalized to the interpolated open rate at V = 0 mV.

Again, both systems follow a common trend with the mean open time being voltage-independent τ_O (Fig. 3A) from Vpu_{1-32}. For Vpu_{1-81}, the open time of the main-conductance state is $\tau_{O,main} = 0.46 \pm 0.03$s and $\tau_{O,sub}$ is 0.43 ± 0.06s. Channels assembled by Vpu_{1-32} possess only slightly longer open times with $\tau_{O,main} = 0.50 \pm$
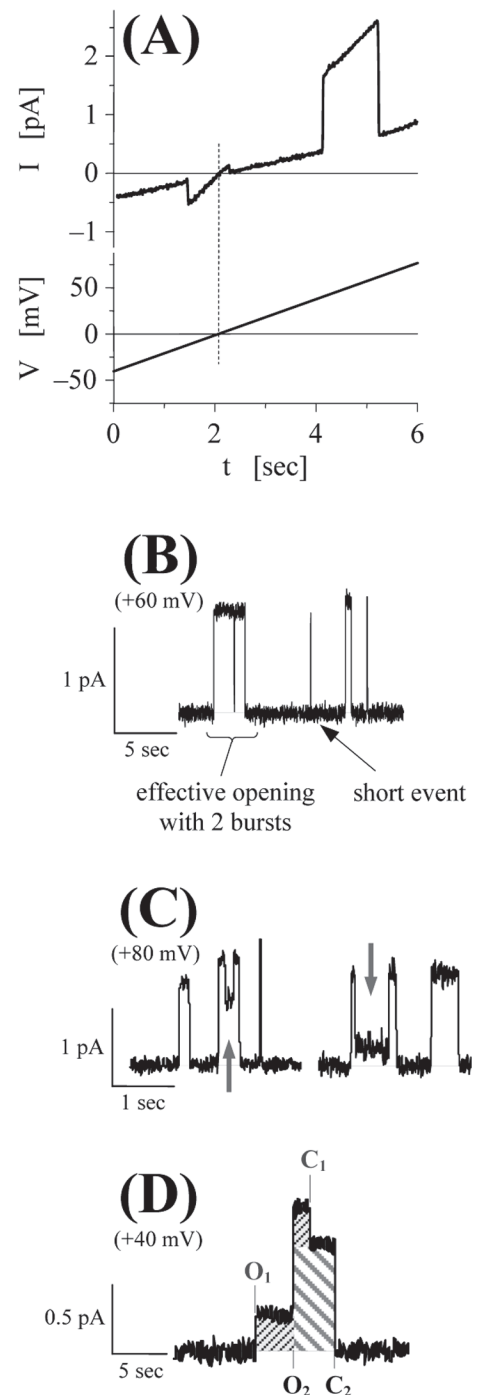
Figure 2: (**A**) Channel open event at V = 0 mV as observed during voltage ramp measurements with Vpu_{1-32} between ±100 mV. (**B**) Two examples of the rare transitions between different conductance states. (**C**) Separation of a multiple channel event in its single channel portions. (**D**) 'Effective opening' event for Vpu_{1-32} with two bursts, separated by a shut event.

0.04s and $\tau_{O,sub} = 0.46 \pm 0.05$s. In contrast to τ_O, all k_{+i} show a voltage dependence (Fig. 3B). The relative rates for Vpu_{1-32} drop from about 3.5 at -150 mV and rise again after passing V = 0 mV. Beyond +100 mV, the k_{+i} begin to level off at around 2.0. Within the smaller voltage range of investigation for Vpu_{1-81} (±60 mV) such channels also show an increase of k_{+i} with raising electric potential. The asymmetric open rate indicates the existence of asymmetrically reconstituted channels as those could not be obtained with an isotropic ensemble of channels.
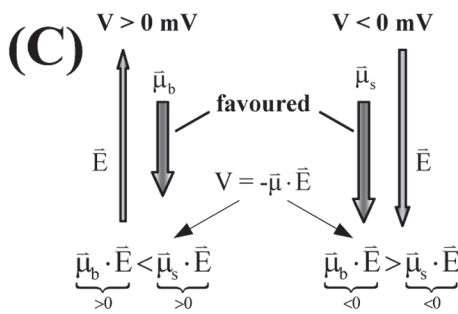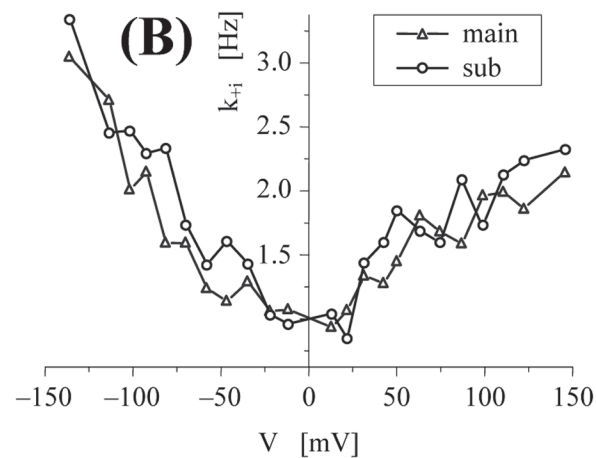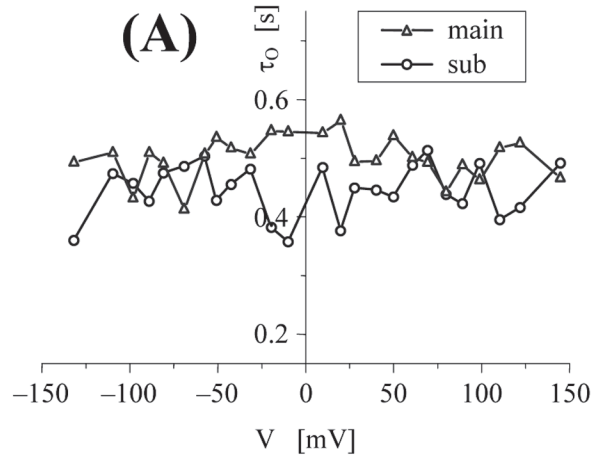
Discussion

The similarity of the recordings, the distribution of conductance states (see Fig. 1C and D), as well as the ohmic ion conducting for both full length Vpu_{1-81} and the TM domain representing peptide Vpu_{1-32} demonstrate that channels formed solely by the TM part of Vpu follow the behavior of assemblies of Vpu_{1-81}. For this reason, investigations on Vpu_{1-32} can be regarded as case studies to extend the understanding of general principles of the construction of ion channels formed by full length Vpu. It has been reported that the existence of the cytoplasmic part of the protein modulates channel characteristics such as elongated open times for the full length protein (34). In the present study, and under the experimental condition reported, only marginal differences in the open time of the main and sub conductance states between Vpu_{1-82} and Vpu_{1-32} have been observed.

It is the working hypothesis in this paper that the bundle once formed remains a bundle and that changes in the conductance are due to gating rather than an appearance or disappearance of the oligomeric state.

It has been proposed that Vpu forms weakly cation-selective ion channels (35). One potential source of the multiple conductance states can be assigned to differences between cationic and anionic currents, since anions and cations flow in opposite directions down the electrochemical potential and both cannot flow simultaneously. The large number of sub-conductance states may not originate from different oligomeric states. It is unlikely that a large range of oligomeric states exist. With an increasing number of monomers forming the bundle, any selectivity of the resulting channel will vanish. Moreover, defining distinct conductance ranges and determining their open rates reveals an identical asymmetric behavior with respect to the applied voltage for all conductance states (representatively shown for two conductance states in Fig. 3B). Consequently, it is not possible that these conductance states may result from different orientations of some helices within a single bundle. Multiple conductance states have also been reported for gramicidin (33) and attributed to small conformational changes in the channel geometry (36). We have also taken care to derive a pure peptide so that these multiple channels do not result from impurities. Summarizing these considerations, the sub-conductance states are thought to originate from different open state conformations under the current experimental conditions.

It is assumed that the transition of the peptide from TFE into the lipid bilayer results in the proper fold of a helical TM domain and that peptides with an improper fold lead to non-functional assemblies that cannot conduct ions.

Figure 3: Channel gating for Vpu channels. (**A**) Mean open time τ_O of Vpu_{1-32} channels as a function of the applied external potential difference. (**B**) Voltage-dependence of the open rates k_{+i} of Vpu_{1-32} bundles. The rates were normalized to the mean value of ±10 mV. (**C**) Favored helix dipole-moment at applied voltage V > 0 mV and V < 0 mV.

The asymmetric voltage dependence with respect to V = 0 mV of the open rates k_{+i} (i = 1, 2) reported here can also be explained by a straightening of the helices either as individual helix or in a concerted motion of all of them (Fig. 3C). As a kinked TM helix straightens, the C=O and N-H bonds take up a more parallel alignment to the helix axis and the overall helix dipole-moment increases. If the vector of an electric field is parallel to the dipole-moment a stretched helix becomes energetically more favorable than the kinked conformation whereas an anti-parallel orientation favors the kinked form in a voltage-dependent manner (Fig. 3C).

At the current state, we do not have an explanation of the biphasic behavior of voltage activation. The tendency of ions to follow an electric field leads to an additional driving force for the gating that rises at higher voltages, regardless of its polarity. It can only be speculated that ions in the channel lumen, are pulled towards the pore center by the field, exert a slight outward force on the helices, and facilitating the opening of a channel. At negative voltages, the interaction of the electric field with the helix dipole-moments and the force exerted by ions combine to increase the open rates. At positive voltages, the forces partially cancel, resulting in the leveling off of the k_{+i} beyond +100 mV (Fig. 3B).

The mean open times $\tau_{O,i}$ and shut rates $k^{-1} = \tau_{O,i}^{-1}$ (Fig. 3A) are voltage independent; that is, channel closing must be driven by a force not being based on an interaction with an electric gradient, which could be most likely the intrinsic lateral pressure of the lipid bilayer.

Conclusions

The presented data suggest that channels formed by the small peptide Vpu$_{1-32}$, mainly consisting of the TM part of Vpu, follow similar characteristics as those of Vpu$_{1-81}$ under the reported experimental conditions. The presented data are interpreted on the basis of stable bundles that undergo a gating process. The biphasic voltage activation is indicative for interaction of the dipole moments of the channel forming TM helices with an external electric field influences channel opening.

It is suggested that the lateral pressure of the bilayer matrix affects closing. Therefore, it is further hypothesized that Vpu channels are able to sense lipid composition by the lateral membrane pressure and can respond to environmental changes as they progress through the compartments of infected cells.

Acknowledgement

References and Footnotes

1. K. Strebel, T. Klimkait, and M. A. Martin. *Science 241*, 1221-1223 (1988).
2. E. A. Cohen, E. F. Terwilliger, J. G. Sodroski, and W. A. Haseltine. *Nature 334*, 532-534 (1988).
3. D. Trono. *Cell 82*, 189-192 (1995).
4. M. Montal. *FEBS Lett. 552*, 47-53 (2003).
5. W. B. Fischer. *FEBS Lett. 552*, 39-46 (2003).
6. S. J. Opella, S. H. Park, S. Lee, D. H. Jones, A. A. Nevzorov, M. F. Mesleh, A. A. Mrse, F. M. Marassi, M. Oblatt-Montal, M. Montal, S. Bour, and K. Strebel. In *Viral Membrane Proteins: Structure, Function and Drug design*, pp 147-163. Ed., W. B. Fischer. Kluwer Academic/Plenum Publishers, New York (2004).
7. V. Wray and U. Schubert. In *Viral Membrane Proteins: Structure, Function and Drug Design*, pp 165-175. Ed., W. B. Fischer. Kluwer Academic/Plenum Publishers, New York (2005).
8. R. L. Willey, F. Maldarelli, M. A. Martin, and K. Strebel. *J Virol 66*, 7193-7200 (1992).
9. T. Kimura, M. Nishikawa, and A. Ohyama. *J Biochem 115*, 1010-1020 (1994).

10. U. Schubert, S. Bour, A. V. Ferrer-Montiel, M. Montal, F. Maldarelli, and K. Strebel. *J Virol 70*, 809-819 (1996).

11. T. Klimkait, K. Strebel, M. D. Hoggan, M. A. Martin, and J. M. Orenstein. *J Virol 64*, 621-629 (1990).

12. U. Schubert, A. V. Ferrer-Montiel, M. Oblatt-Montal, P. Henklein, K. Strebel, and M. Montal. *FEBS Lett 398*, 12-18 (1996).

13. K. Hsu, J. Seharaseyon, P. Dong, S. Bour, and E. Marbán. *Molec Cell 14*, 259-267 (2004).

14. K. C. Duff and R. H. Ashley. *Virology 190*, 485-489 (1992).

15. L. J. Holsinger, D. Nichani, L. H. Pinto, and R. A. Lamb. *J Virol 68*, 1551-63 (1994).

16. K. Shimbo, D. L. Brassard, R. A. Lamb, and L. H. Pinto. *Biophys J 70*, 1335-1346 (1996).

17. R. A. Lamb and L. H. Pinto. *Virology 229*, 1-11 (1997).

18. J. A. Mould, R. G. Paterson, M. Takeda, Y. Ohigashi, P. Venkataraman, R. A. Lamb, and L. H. Pinto. *Dev Cell 5*, 175-184 (2003).

19. B. Plugge, S. Gazzarrini, M. Nelson, R. Cerana, J. L. Van Etten, C. Derst, D. DiFrancesco, A. Moroni, and G. Thiel. *Science 287*, 1641-1644 (2000).

20. D. Pavlovic, D. C. A. Neville, O. Argaud, B. Blumberg, R. A. Dwek, W. B. Fischer, and N. Zitzmann. *Proc Natl Acad Sci USA 100*, 6104-6108 (2003).

21. W. Lu, B.-J. Zheng, K. Xu, W. Schwarz, L. Du, C. K. L. Wong, J. Chen, S. Duan, V. Deubel, and B. Sun. *Proc Natl Acad Sci USA 103*, 12540-12545 (2006).

22. J. V. Melton, G. D. Ewart, R. C. Weir, P. G. Board, E. Lee, and P. W. Gage. *J Biol Chem 277*, 46923-46931 (2002).

23. L. Wilson, C. McKinlay, P. Gage, and G. Ewart. *Virology 330*, 322-331 (2004).

24. E. Tiganos, J. Friborg, B. Allain, N. G. Daniel, X.-J. Yao, and E. A. Cohen. *Virology 251*, 96-107 (1998).

25. G. A. Woolley and B. A. Wallace. *J Membr Biol 129*, 109-136 (1992).

26. B. Bechinger. *J Membr Biol 156*, 197-211 (1997).

27. G. Boheim, W. Hanke, and G. Jung. *Biophys Struct Mech 9*, 181-191 (1983).

28. W. Hanke, C. Methfessel, H.-U. Wilmsen, E. Katz, G. Jung, and G. Boheim. *Biochim Biophys Acta 727*, 108-114 (1983).

29. A. S. Arseniev, L. L. Barsukov, V. F. Bystrov, A. L. Lomize, and Y. A. Ovchinnikov. *FEBS Lett 186*, 168-174 (1985).

30. M. Montal and P. Müller. *Proc Natl Acad Sci USA 69*, 3561-3566 (1972).

31. W. Römer, Y. H. Lam, D. Fischer, A. Watts, W. B. Fischer, P. Göring, R. B. Wehrspohn, U. Gösele, and C. Steinem. *J Am Chem Soc 126*, 16267-16274 (2004).

32. P. Matsudaira. *J Biol Chem 262*, 10035-10038 (1987).

33. D. Busath and G. Szabo. *Nature 294*, 371-373 (1981).

34. C. Ma, F. M. Marassi, D. H. Jones, S. K. Straus, S. Bour, K. Strebel, U. Schubert, M. Oblatt-Montal, M. Montal, and S. J. Opella. *Prot Sci 11*, 546-557 (2002).

35. G. D. Ewart, T. Sutherland, P. W. Gage, and G. B. Cox. *J Virol 70*, 7108-7115 (1996).

36. D. W. Urry, S. Alonso-Romanowski, C. M. Venkatachalam, T. L. Trapane, and K. U. Prasad. *Biophys J 46*, 259-266 (1984).